Enhancement of coherent charge oscillations in coupled quantum wells by femtosecond pulse shaping

A. M. Weiner

School of Electrical Engineering, Purdue University, West Lafayette, Indiana 47907-1285

Received March 8, 1994; revised manuscript received June 1, 1994

The effect of femtosecond pulse shaping on the amplitude of optically excited coherent charge oscillations in degenerate coupled quantum wells is analyzed. In the absence of dephasing, the final oscillating polarization after the end of the shaped pulse depends only on the optical power spectrum; pulse shaping cannot enhance the final coherent polarization. However, appropriately shaped ultrashort pulses can lead to strong peaks in the oscillating dipole during the laser pulse. I present a method for designing waveforms capable of producing strong peaks in the coherent polarization and illustrate this approach by giving several examples. The computed results indicate the possibility of enhancing the peak oscillating dipole (and hence the resulting terahertz emission) by at least a factor of 4.

1. INTRODUCTION

Coherent quantum-mechanical charge oscillations in GaAs–GaAlAs heterostructures have been recently observed in a series of elegant experiments.[1–8] These oscillations are excited by ultrashort-pulse excitation of quantum-well or superlattice samples and have been detected by both four-wave mixing and terahertz (THz) emission. Because these coherent charge oscillations arise from time-varying quantum-mechanical interference between nearly degenerate wave functions simultaneously excited by absorption of the ultrashort pulse, they are closely related to the quantum-mechanical wave-packet motions widely observed in atomic and molecular systems. For this reason, as well as because of potential device applications, these experiments have aroused considerable interest.

Two recent studies have explored the effect of using simple sequences of femtosecond pulses on the excitation of coherent charge oscillations in semiconductor quantum wells and on the resulting THz emission.[4,5] These investigations have clarified the role of the optical phase in exciting charge oscillations and have demonstrated the ability either to reinforce or to suppress charge oscillations by controlling the pulse timing and phase. However, neither of these experiments evidenced an increase in the peak charge oscillation amplitude as a result of using pulse sequences rather than individual ultrashort pulses. In this paper I analyze the efficiency of charge oscillations excited by specially shaped femtosecond pulse waveforms and pulse sequences and explain why experiments have not resulted in enhanced oscillation amplitudes. I then discuss how considerable oscillation enhancement can be achieved and derive several examples of ultrafast waveforms that would be suitable for this purpose. The waveforms shown could readily be generated by existing programmable pulse-shaping techniques; therefore experiments based on these theoretical results should be immediately feasible.

This study is closely related to the emerging field of coherent control, in which researchers seek to tailor wave-packet motions by manipulating constructive and destructive quantum-mechanical interferences in molecular systems.[9–13] Coherent control could ultimately lead to optical manipulation of chemical reactions and in the shorter term should make possible the preparation of well-defined quantum-mechanical states for precise spectroscopic determination of molecular Hamiltonians. Two main approaches for coherent control have been suggested. One approach uses specially tailored ultrashort pulses with features faster than the natural molecular vibrational periods to manipulate quantum-mechanical interferences[9–12]; the other approach utilizes the interference of multiple, phase-coherent laser frequencies.[13] Despite considerable interest and intense theoretical efforts experimentation is still at an early stage, and only a few rather simple experimental demonstrations have been reported.[14–19]

In this paper I describe the possibility of using specially designed multiple-quantum-well structures as a laboratory for testing ultrashort-pulse coherent control concepts. One motivation for using layered semiconductors as a coherent control laboratory is the ability to control the Hamiltonian through the epitaxial growth process and band-gap engineering. Therefore one may have more knowledge of and more control over the Hamiltonian than one has in studies of complex molecules, in which imprecise knowledge about the Hamiltonian is often one of the major difficulties. A second exciting motivation is that the ability to manipulate charge motions within layered compound semiconductors could lead to the realization of new classes of optoelectronic devices capable of processing ultrafast optical signals.

Note that an early version of this study was previously presented in abstract form.[20] In addition, another group simultaneously considered the application of coherent control concepts to alleviate inhomogeneous broadening effects in double-quantum-well systems.[21] One difference in the theoretical approaches taken in these two papers is worth noting: in Ref. 21 the authors

0740-3224/94/122480-12$06.00

utilize an iterative optimization technique to arrive at the desired optimum laser waveform; in the present paper and in Ref. 20 I write down a formula for a near-optimum pulse shape by inspection (although computer calculation is still required for evaluation of this formula).

The structure of this paper is as follows. In Section 2 I summarize experiments in which ultrashort pulses were used to excite charge oscillations resulting in THz emission from semiconductor heterostructure. Then, in Section 3, I focus on experiments that involve coupled pairs of quantum wells excited by femtosecond pulse sequences, with an emphasis on the amplitude of the charge oscillations achieved. I put forth a simple analytical expression that explains why experiments to date have not resulted in enhancements in the oscillation amplitude. In Section 4 I discuss opportunities for increasing the magnitude of the charge motion through femtosecond pulse shaping. In particular, I describe a methodology for designing femtosecond optical waveforms that maximizes the peak oscillation amplitude for a fixed initial laser pulse energy and give several illustrative examples. In Section 5 I discuss additional issues relevant to experimental implementation of these ideas and describe possible extensions to coherent control of charge motions in three-quantum-well systems and superlattices. Finally, in Section 6 a summary is presented.

2. THEORETICAL BACKGROUND

In this section we consider charge oscillations in double-coupled quantum wells (DCQW's) excited by absorption of an ultrashort laser pulse. The situation is shown schematically in Fig. 1. As a prototypical sample we consider a DCQW design [Fig. 1(a)], which was described in detail in connection with several pioneering experiments performed at AT&T Bell Laboratories.[1,2] One wide and one narrow GaAs quantum well are separated by a thin AlGaAs barrier region. An electric field is applied to tilt the energy bands. When the lowest electron energy levels in the two wells line up, the two wells couple effectively, which leads to an energy-level splitting and a delocalization of the wave functions across the two wells. Note that the hole energy levels remain nondegenerate, and therefore the hole wave functions are not coupled between the two wells. Thus a short optical pulse can be excited from the valence band in one particular well into a conduction-band superposition state initially localized in the same well. Because of the quantum-mechanical coupling, however, this results in an oscillatory wave-packet motion of the electron back and forth from one well to the other. Such oscillatory charge motions were observed by means of several experimental techniques, such as four-wave mixing[1] and detection of THz radiation.[2]

In this analysis we are most interested in enhancing the charge oscillation by using specially shaped laser-excitation waveforms. Techniques for generating such shaped waveforms, and experiments to date that use shaped pulses for driving charge oscillations, are described in Section 3.

In addition to the DCQW samples discussed above, experiments were also reported in which ultrashort-pulse excitation resulted in charge oscillations because of interference between light- and heavy-hole excitons within a single quantum well.[3] The analysis below applies not only to charge oscillations in DCQW structures but also to oscillations that involve light- and heavy-hole excitons in a single well.

Detection of THz emission is one of the cleanest ways to observe the charge oscillation dynamics because this technique is insensitive to phenomena that do not involve actual charge motions. Motion of the electrons between the two wells leads to an oscillating dipole moment, which then radiates at the (THz) oscillation frequency. The radiated electric field is proportional to the second derivative of the coherent time-varying polarization P:

$$E_{\mathrm{THZ}}(t) \sim \partial^2 P(t)/\partial t^2 . \tag{1}$$

The resulting THz radiation is detected by standard techniques, e.g., by use of an ultrashort laser pulse to gate an ultrafast photoconductive antenna.[22,23]

Recently Luo *et al.* published a density-matrix analysis of induced charge oscillations in DCQW's.[24] They treated the DCQW as a three-level system and included a damping term representing the dephasing of the coupled quantum wells. Their analysis focused on the use of phase-locked pulse pairs for controlling the charge oscillation dynamics, and, by comparing their theory with experimental results obtained with phase-locked pulse pairs,[4] they verified the adequacy of the three-level model for explaining the charge oscillation dynamics. Their results also showed that most of the important physics in the experiments could be understood without inclusion of the dephasing terms. After solving for the density matrix, they obtained the coherent polarization $P(t)$ by means of the following expression:

$$P(t) \sim \rho_{11}(t)(\mu_{33} - \mu_{11}) + \rho_{22}(t)(\mu_{33} - \mu_{22}) - 2\mu_{12}\,\mathrm{Re}[\rho_{12}(t)], \tag{2}$$

where ρ_{11} and ρ_{22} are the populations of the coupled conduction subbands and μ_{ij} is the dipole moment between states i and j. The first two terms in relation (2) represent an electric-field-induced optical rectification that arises because excitons are created in a polarized state; these terms follow the integral of the incident optical pulses and lead to a fast transient in the THz emission. The last term in relation (2) is associated with oscillatory

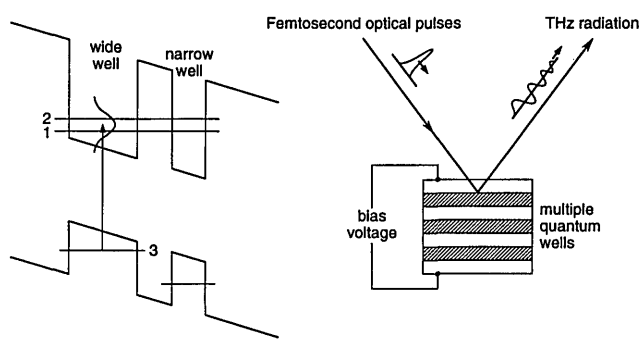

Fig. 1. (a) Schematic energy-level diagram of a DCQW system, (b) schematic representation of THz radiation induced by femtosecond excitation of the coupled-quantum-well system.

charge motions between the coupled conduction subbands in the narrow and the wide wells.

Below we focus our attention on this last, oscillatory term, and we ignore the field-induced optical rectification terms. Neglecting the rectification terms is justified for two reasons: (a) for low enough electric fields the oscillatory term can dominate the field-induced rectification term,[2] and (b) the use of appropriately shaped femtosecond waveforms can enhance the peak THz emission associated with the oscillatory polarization, whereas the THz emission associated with rectification is expected to be significantly reduced because of the longer durations of the shaped excitation pulses. With respect to point (b), this effect is similar to the results of experiments in which multiple-pulse sequences were used to excite optical phonons in molecular crystals through impulsive stimulated Raman scattering.[14,15] In particular, in these multiple-pulse Raman scattering experiments, the ratio of the phonon-scattering peaks to the unwanted scattering arising from the instantaneous (electronic) Kerr nonlinearity was significantly enhanced relative to experiments with single femtosecond excitation pulses.

In the analysis below, dephasing effects are neglected; this allows us to concentrate on the effects of pulse shaping on the coherent charge oscillation. Dephasing of course does occur in semiconductors; for the DCQW's studied experimentally,[2] the dephasing time is several picoseconds for temperatures of ~10 K, compared with a charge oscillation period of ~700 fs. Nevertheless, even without dephasing we can still formulate some important results describing the strength of the charge oscillation excited and can identify opportunities for enhancing the oscillation. In Section 5 we briefly discuss how dephasing would modify the current results.

Because dephasing is not included below, we can express our analysis in terms of the wave functions (as opposed to the density matrix). We write the wave function as follows:

$$|\Psi\rangle = c_1(t)\exp(-iE_1t/\hbar)|\phi_1\rangle + c_2(t)\exp(-iE_2t/\hbar)|\phi_2\rangle + c_3(t)|\phi_3\rangle. \quad (3)$$

Here $|\phi_1\rangle$ and $|\phi_2\rangle$ are the wave functions of the coupled conduction subbands and $|\phi_3\rangle$ is the valence-band wave function (e.g., the heavy hole). E_1 and E_2 are the energies of the conduction subbands, and the ground-state energy E_3 is taken to be zero. We assume that initially only the ground state is populated, so that, before the occurrence of the laser pulse, $c_3^{(0)} = 1$, $c_1^{(0)} = c_2^{(0)} = 0$. We obtain the charge oscillation dynamics by solving the Schrödinger equation, with the optical field being included as a perturbation term, as follows:

$$i\hbar\frac{\partial|\Psi\rangle}{\partial t} = H_0|\Psi\rangle - \mu e_L(t)|\Psi\rangle, \quad (4)$$

where

$$e_L(t) = a_L(t)\exp(-i\Omega_L t) + a_L{}^*(t)\exp(i\Omega_L t). \quad (5)$$

Here $e_L(t)$ is the total laser field (which may be specially shaped; see Section 3), $a_L(t)$ is a slowly varying envelope function, Ω_L is the center frequency of the optical pulse, and μ is dipole moment operator.

The first-order perturbation solutions for the wave-function amplitudes are easily obtained:

$$c_1^{(1)}(t) = \frac{i\mu_{13}}{\hbar}\int^t dt' e_L(t')\exp(iE_1t'/\hbar),$$

$$c_2^{(1)}(t) = \frac{i\mu_{23}}{\hbar}\int^t dt' e_L(t')\exp(iE_2t'/\hbar). \quad (6)$$

We can write these formulas in a more convenient form by introducing the notation

$$\tilde{\omega}_1 = (E_1/\hbar) - \Omega_L,$$

$$\tilde{\omega}_2 = (E_2/\hbar) - \Omega_L. \quad (7)$$

The result, in which only the terms near resonance are kept, is as follows:

$$c_1^{(1)}(t) = \frac{i\mu_{13}}{\hbar}\int^t dt' a_L(t')\exp(i\tilde{\omega}_1t'),$$

$$c_2^{(2)}(t) = \frac{i\mu_{23}}{\hbar}\int^t dt' a_L(t')\exp(i\tilde{\omega}_2t'). \quad (8)$$

Finally we solve for the coherent polarization:

$$P(t) = \langle\Psi|\mu|\Psi\rangle = \mu_{21}c_2{}^*c_1\exp(i\omega_{21}t) + \text{c.c.}$$
$$= \frac{\mu_{21}\mu_{13}\mu_{23}{}^*}{\hbar^2}\exp(i\omega_{21}t)\int^t dt' a_L(t')\exp(i\tilde{\omega}_1t') \times \int^t dt' a_L{}^*(t')\exp(-i\tilde{\omega}_2t') + \text{c.c.}, \quad (9)$$

where $\omega_{21} = (E_2 - E_1)/\hbar$ is the frequency difference between the two conduction-band levels and c.c. denotes the complex conjugate. Equation (9) shows that the coherent polarization oscillates at a frequency ω_{21}, as expected. Furthermore, the amplitude of the polarization is proportional to the product $c_1(t)c_2{}^*(t)$. The coefficients $c_1(t)$ and $c_2{}^*(t)$ in turn resemble the Fourier transform of the laser field (evaluated at the conduction-subband frequencies), with the difference that the integrals extend only to the time t at which $P(t)$ is evaluated.

The expression for the polarization simplifies further for times longer than the laser pulse duration, for which we can set $t \to \infty$. The result is as follows:

$$P(t) = \frac{\mu_{21}\mu_{13}\mu_{23}{}^*}{\hbar^2}\exp(i\omega_{21}t)\int_{-\infty}^{\infty} dt' a_L(t')\exp(i\tilde{\omega}_1t') \times \int_{-\infty}^{\infty} dt' a_L{}^*(t')\exp(-i\tilde{\omega}_2t') + \text{c.c.}$$
$$= \frac{\mu_{21}\mu_{13}\mu_{23}{}^*}{\hbar^2}\exp(i\omega_{21}t)A_L(\tilde{\omega}_1)A_L{}^*(\tilde{\omega}_2) + \text{c.c.} \quad (10)$$

Here $A_L(\omega)$ is the Fourier transform of electric-field envelope $a_L(t)$. For times after completion of the exciting laser pulse, the terminal coherent polarization is proportional to the real part of the product of the spectral amplitudes $A_L(\tilde{\omega}_1)A_L{}^*(\tilde{\omega}_2)$ at the two conduction-subband energies. This is an important point, to which we return in Section 3 when we discuss the efficiency of charge oscillations excited by femtosecond pulse sequences. Also note from Eq. (10) that the phase of the oscillating polarization is directly related to the phase of the spectral amplitudes. Thus, if we write $A_L(\omega) = |A_L(\omega)|\exp[i\phi(\omega)]$, then we can rewrite the terminal polarization as

$$P(t \to \infty) \sim |A_L(\tilde{\omega}_1)|\,|A_L(\tilde{\omega}_2)|\cos[\omega_{21}t + \phi(\tilde{\omega}_1) - \phi(\tilde{\omega}_2)]. \quad (11)$$

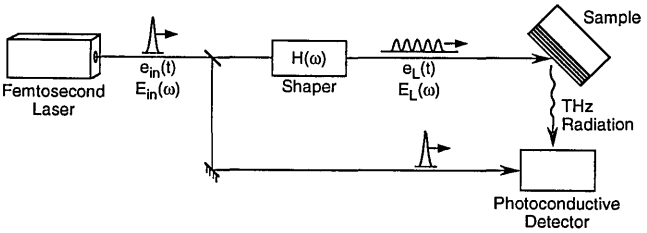

Fig. 2. Schematic diagram of experiments in which shaped femtosecond waveforms excite charge oscillations, resulting in THz emission. The input pulse $e_{in}(t)$ [with spectrum $E_{in}(\omega)$] is reshaped by a linear filter characterized by a frequency response $H(\omega)$. The shaped waveform or pulse sequence $e_L(t)$ [with spectrum $E_L(\omega)$] is then absorbed by the DCQW sample. We are interested in finding the optimum filter $H(\omega)$ that, for a given pulse duration and energy from the laser, yields the highest peak charge oscillation amplitude.

If the relative phases of the two spectral amplitudes are changed, the phase of the terminal coherent polarization is changed by the same amount.

3. CHARGE OSCILLATIONS IN DOUBLE-COUPLED QUANTUM WELLS EXCITED BY FEMTOSECOND PULSE SEQUENCES

We are interested in charge oscillations in DCQW's excited by femtosecond pulse sequences or specially shaped femtosecond waveforms, as shown in Fig. 2. We assume that individual femtosecond pulses from a mode-locked laser are converted into the required pulse sequences or waveforms by means of a linear filter. The linear filter can be implemented by interferometric techniques[16] or by Fourier-transform pulse shaping,[25,26] or by other methods. The filter can be characterized in terms of its frequency response $H(\omega)$, and the shaped output pulse from the filter is related to the input pulse from the laser by the following simple formula:

$$e_L(t) = \frac{1}{2\pi}\int d\omega\, \exp(-i\omega t)H(\omega)E_{in}(\omega), \qquad (12)$$

where

$$E_{in}(\omega) = \int dt\, \exp(i\omega t)e_{in}(t).$$

Here $E_{in}(\omega)$ is the Fourier transform of the input pulse from the laser $e_{in}(t)$, and $E_L(\omega) = H(\omega)E_{in}(\omega)$ is the Fourier transform of the shaped pulse $e_L(t)$. The shaped waveform illuminates the sample, resulting in the emission of THz radiation, which one detects by gating a photoconductive dipole antenna.[22,23]

Below we focus on the amplitude of coherent polarization (and hence THz emission) excited for a given pulse energy at the output of the laser. In particular, we consider the following question: How does the inclusion of the pulse-shaping linear filter affect the charge oscillation amplitude?

From relations (10) and (11) we can immediately conclude that the terminal coherent polarization that results after the laser pulse is finished is not enhanced by pulse shaping (again assuming that dephasing does not play a role). The terminal polarization is proportional to the product of the spectral amplitudes at the conduction-subband energies. For a passive linear filter, $|H(\omega)| \le 1$; therefore the spectral amplitudes cannot be increased by the pulse-shaping process.

This observation is supported by experiments in which femtosecond pulse sequences are used for excitation of charge oscillations in DCQW's.[4,5] In one experiment an interferometer was used to split an incident pulse into a pulse doublet, which was used to excite the coupled-quantum-well sample. Studies of the THz emission as a function of the delay and the phase of the second pulse clearly revealed the importance of the optical phase in reinforcing or canceling the induced charge oscillation.[4,24] For two pulses with the proper relative timing and phase, the peak THz signal generated by the pulse pair is roughly four times as large as the signal generated by one pulse alone (with the second pulse blocked). Note, however, that this is no larger than the peak THz signal that would be obtained with no interferometer at all. For an input pulse $e_{in}(t) = \mathrm{Re}[a_{in}(t)\exp(-i\Omega_L t)]$ the envelope of the electric field emerging from the interferometer is written as

$$a_L(t) = {}^1\!/_2 a_{in}(t) + {}^1\!/_2 a_{in}(t-\tau)\exp(i\Omega_L\tau). \qquad (13)$$

The factor of one half is required because half the input energy emerges from the unused port of the interferometer. Because the coherent polarization excited by a single pulse is proportional to the square of the electric-field amplitude, a single pulse emerging from the interferometer produces only one quarter the polarization induced by the original pulse directly from the laser. Two pulses appropriately phased yield the same coherent polarization as the original pulse from the laser.

Note that one derives the same conclusion by describing the interferometer in terms of its frequency response $H(\omega)$:

$$H(\omega) = \exp(j\omega\tau/2)\cos\left[\frac{(\omega-\Omega_L)}{2}\tau\right]. \qquad (14)$$

We can see that $|H(\omega)| \le 1$, as stated; therefore the terminal coherent polarization is not increased by use of the interferometer. The terminal polarization equals that obtained with $e_{in}(t)$ (no interferometer) when the cosine in Eq. (14) has peaks at both conduction-subband energies. Also note that the polarization induced per unit laser energy incident upon the sample is increased through the filtering process; the interferometer eliminates energy at some of the frequency components that are not useful for creating a coherent polarization.

A second related experiment used a Fourier-transform pulse-shaping setup to generate a train of pulses spaced at the natural charge oscillation frequency.[5] The pulse-shaping apparatus is depicted in Fig. 3 and is described in detail in a number of references.[25–27] A grating and a lens spatially disperse the incident optical-frequency components; a spatially patterned mask is placed at the Fourier plane to manipulate the phase and/or the amplitude of the individual optical frequencies. The second grating and lens recombine the frequencies into a single collimated beam; this yields an output pulse whose shape is determined by the Fourier transform of the

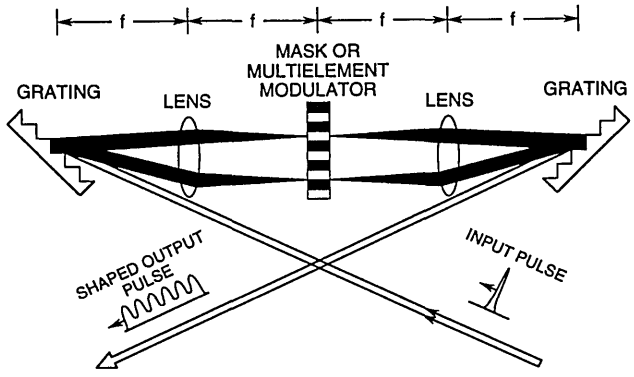

Fig. 3. Fourier-transform pulse-shaping apparatus. Optical-frequency components contained in the input laser pulse are spatially dispersed, filtered, and then spatially recombined. The result is a reshaped output pulse, with the pulse shape being determined by the Fourier transform of the phase and the amplitude pattern transferred from the mask onto the spectrum.

spatial pattern transferred by the mask onto the spectrum. To a good approximation the filter function $H(\omega)$ is equal to an appropriately scaled version of the masking function. For the multiple-pulse experiments of Ref. 5 a specially designed periodic phase mask was used to transform the single input pulse into the desired pulse train without loss of energy. Similar masks were used previously to generate pulse trains for periodic excitation of optical phonons in molecular crystals by impulsive stimulated Raman scattering.[14,15,27] Note that computer-programmable pulse shaping was also demonstrated with multielement liquid-crystal phase[26] and amplitude[28] modulators in place of fixed masks; such programmable pulse shapers will be especially useful for generating the optimized femtosecond waveforms described in Section 4.

The THz signals reported in the experiments of Brener *et al.*[5] are shown in Fig. 4. Figure 4(a) shows the signal that resulted when the DCQW sample was excited by a single femtosecond pulse directly from the laser, whereas Fig. 4(b) shows the data for the case of a femtosecond pulse train generated in the pulse shape. The laser waveforms themselves are also shown for both cases in the insets. Note that the peak THz signal for the multiple-pulse and the single-pulse cases are the same, although the peak optical intensity is much weaker in the multiple-pulse case. Note also that the THz signal does not build up at all during the first several picoseconds of multiple-pulse excitation but then builds up rather abruptly within a few pulse periods. The behavior arises because the phases of the individual pulses in the sequence were not all the same in this experiment (this is an inevitable consequence of using phase-only masks to generate the pulse train[27]). During the first part of the pulse train the incident pulses are out of phase, and no significant charge oscillation is induced. Near $t = 0$ several pulses are apparently in phase, and the charge motion then builds up rapidly.

This observed rapid buildup motivates us to ask the following question: Can laser pulse shapes be designed that would significantly enhance the amplitude of the charge oscillation and hence the radiated THz signal? We have already seen that the terminal coherent polarization will not be improved through pulse shaping. However, the coherent polarization can be enhanced while the laser pulse is still on. In Section 4 I show how to design shaped laser waveforms that should significantly enhance the peak polarization compared with a single, unshaped pulse.

4. ENHANCING THE PEAK CHARGE OSCILLATIONS THROUGH PULSE SHAPING

Relations (10) and (11) show that the terminal coherent polarization as $t \rightarrow \infty$ reaches a value determined only by the power spectrum of the shaped pulse. In contrast, Eq. (9) shows that the coherent polarization $P(\tau)$ at a particular time τ during the laser pulse is determined by the Fourier transform of the electric field truncated at time τ. Therefore, to optimize $P(\tau)$, one must choose a shaped pulse so that the Fourier transform of the truncated field is enhanced at the conduction-subband energies. Such a pulse will excite a polarization that first peaks and then relaxes to the terminal value dictated by the power spectrum. The peak polarization at time τ may be significantly higher than is possible with an unshaped pulse of the same initial energy.

We wish to design a pulse-shaper filter $H(\omega)$ that optimizes the polarization at a chosen time τ. We proceed by defining a linear operator $\mathbf{T}_\omega(t)$, which we use to rewrite Eq. (9) for the coherent polarization in the following simplified form:

$$P^{(2)}(t) \sim \mathrm{Re}\{\exp(i\omega_{21}t)[\mathbf{T}_{\tilde{\omega}_1}(t)\cdot\mathbf{H}][\mathbf{T}_{\tilde{\omega}_2}(t)\cdot\mathbf{H}]^*\}, \quad (15a)$$

where

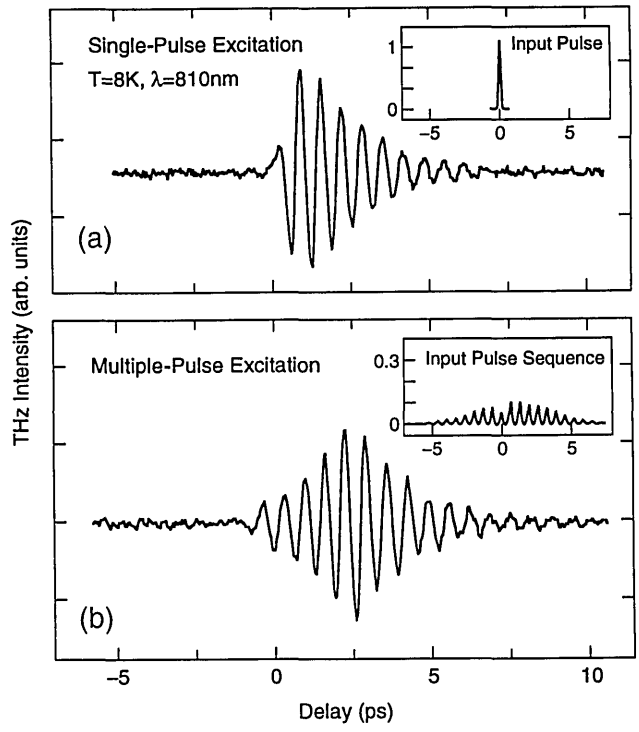

Fig. 4. Data from Brener *et al.*[5] showing THz signals from DCQW's excited (a) by single femtosecond pulses and (b) by femtosecond pulse sequences generated by a Fourier-transform pulse-shaping apparatus. The peak THz emission (and hence the peak coherent polarization) is approximately the same for the two cases.

$$\mathbf{T}_\omega(t)\cdot\mathbf{H}=\int^{t} e_L(t')\exp(i\omega t')\mathrm{d}t'. \tag{15b}$$

This formulation has the advantage that for a given t the operator $\mathbf{T}_\omega(t)$ can easily be calculated by performance of a series of matrix multiplications. Then, after $\mathbf{T}_\omega(t)$ is obtained, one can choose a suitable $H(\omega)$ that optimizes $P(t)$ in relations (15). We recall that the resulting shaped laser pulse $e_L(t)$ is given by the Fourier transform of the input spectrum multiplied by the filter response $H(\omega)$.

Before we calculate $\mathbf{T}_\omega$, let us first briefly discuss its significance. From Eq. (15b), we obtain the product $\mathbf{T}_\omega(\tau)\cdot\mathbf{H}$ by multiplying $H(\omega)$ by the input spectrum $E_{\mathrm{in}}(\omega)$, performing an inverse Fourier transform to obtain the shaped laser field $e_L(t)$, truncating the shaped field at time τ, and then performing a final (forward) Fourier transform. If we then evaluate $\mathbf{T}_\omega(\tau)\cdot\mathbf{H}$ at the conduction-subband frequencies $\tilde{\omega}_1$ and $\tilde{\omega}_2$, we can immediately obtain the coherent polarization $P^{(2)}(\tau)$ at time τ by using relation (15a).

The computation proceeds as follows. We write

$$\mathbf{T}_\omega(\tau)\cdot\mathbf{H}=[\mathbf{FT}\cdot\mathbf{TR}(\tau)\cdot\mathbf{IFT}\cdot\mathbf{E}_{\mathrm{in}}]\cdot\mathbf{H}, \tag{16}$$

where **FT** and **IFT** are the forward and the inverse Fourier-transform operators, $\mathbf{E}_{\mathrm{in}}$ represents the input spectrum $E_{\mathrm{in}}(\omega)$, and $\mathbf{TR}(\tau)$ is a time-domain operator that truncates the electric field for times $t>\tau$. The filter $\mathbf{H}$ is taken as an N-element column vector; the other operators are square $(N\times N)$ matrices. In particular, we write

$$\mathbf{H}_j=H(\omega_j), \tag{17a}$$

$$(\mathbf{E}_{\mathrm{in}})_{jk}=E_{\mathrm{in}}(\omega_j)\delta_{jk}, \tag{17b}$$

$$\mathbf{TR}_{jk}(\tau)=\begin{cases}\delta_{jk} & \text{for } t_j\le\tau\\ 0 & \text{for } t_j>\tau\end{cases}, \tag{17c}$$

$$\mathbf{FT}_{jk}=\exp[i(2\pi jk/N)], \tag{17d}$$

$$\mathbf{IFT}_{jk}=\frac{1}{N}\exp[-i(2\pi jk/N)]. \tag{17e}$$

Here δ_{jk} is the Kronecker delta function ($\delta_{jk}=1$ for $j=k$, $\delta_{jk}=0$ for $j\neq k$), and ω_j and t_j represent the sample values of ω and t, respectively. For a given τ the operator $\mathbf{T}_\omega(\tau)=\mathbf{FT}\cdot\mathbf{TR}(\tau)\cdot\mathbf{IFT}\cdot\mathbf{E}_{\mathrm{in}}$ is an $N\times N$ matrix. However, because we need to know $\mathbf{T}_\omega$ only at frequencies $\tilde{\omega}_1$ and $\tilde{\omega}_2$, we need to compute only two rows of the $\mathbf{T}_\omega$ matrix.

Next we discuss examples of the present calculations. Except when otherwise noted, our assumptions are as follows. The input pulse $e_{\mathrm{in}}(t)$ is taken as a Gaussian with a full width at half-maximum (FWHM) duration of 100 fs and with a center frequency centered between the two conduction-subband levels $[\Omega_L=(E_1+E_2)/2\hbar]$. The frequency separation of the conduction subbands $(\omega_{21}/2\pi)$ is set to 2 THz. We assume that the pulse-shaping filter is implemented by use of a 128-element liquid-crystal modulator array within a Fourier-transform pulse-shaping apparatus.[26] Each modulator element corresponds to a frequency spread $\delta f=0.05$ THz. Thus the modulator array accommodates a total frequency span of 6.4 THz, which is enough to pass most (but not all) of the assumed input pulse spectrum. Optical-frequency components that fall outside this window are blocked by a hard aperture. The filter $H(\omega)$ is modeled as a 256-element vector. Of these the central 128 elements correspond to the 128 modulator pixels; the first 64 pixels and the last 64 pixels are set to zero to account for the hard aperture.

Computed values of the $\mathbf{T}_\omega(\tau)$ operator are plotted in Fig. 5. Figure 5(a) shows $\mathbf{T}_\omega(\tau\to\infty)$ for frequencies $\omega=\tilde{\omega}_1$ and $\omega=\tilde{\omega}_2$, in addition to the input spectrum $E_{\mathrm{in}}(\omega)$ (as modified by the finite window of the modulator array). In this case $\mathbf{T}_\omega$ are simply delta functions placed at frequencies $\tilde{\omega}_1$ and $\tilde{\omega}_2$, respectively, with a peak value equal to $E_{\mathrm{in}}(\omega)$ at those frequencies. Thus $\mathbf{T}_{\tilde{\omega}_1}(t\to\infty)\cdot\mathbf{H}=H(\tilde{\omega}_1)E_{\mathrm{in}}(\tilde{\omega}_1)$, and similarly for $\tilde{\omega}_2$. In this limit the coherent polarization depends only on the spectral amplitudes of the shaped laser pulse at frequencies $\tilde{\omega}_1$ and $\tilde{\omega}_2$, as in Eq. (10); pulse shaping cannot enhance the charge oscillation for $\tau\to\infty$, as was discussed above. Figure 5(b) shows $|\mathbf{T}_{\tilde{\omega}_1}|$ and $|\mathbf{T}_{\tilde{\omega}_2}|$ for τ set to 2.5 ps. Now the $\mathbf{T}_\omega$ values broaden out as a function of frequency and develop pronounced pedestals, although the functions are stilled peaked at the same frequencies as before. The phase of the $\mathbf{T}_\omega$ operator can be quite complicated, as shown in Figs. 5(c) and 5(d) for $\omega=\tilde{\omega}_1$ and $\omega=\tilde{\omega}_2$, respectively. Because of the broadening of $\mathbf{T}_\omega$, the product $\mathbf{T}_{\tilde{\omega}_1}\cdot\mathbf{H}$, for example, now involves a weighted sum of $H(\omega)$ in the vicinity of $\tilde{\omega}_1$. For suitable $H(\omega)$ this product can be larger than without pulse shaping, and therefore the polarization in relations (15) can be enhanced in this case of finite τ.

One favorable choice for $H(\omega)$ is as follows:

$$H(\omega)=\begin{cases}\mathbf{T}_{\tilde{\omega}_1}(\tau)/|\mathbf{T}_{\tilde{\omega}_1}(\tau)| & \omega<\Omega_L\\ \mathbf{T}_{\tilde{\omega}_2}(\tau)/|\mathbf{T}_{\tilde{\omega}_2}(\tau)| & \omega>\Omega_L\end{cases}. \tag{18}$$

In this case $H(\omega)$ is a phase-only filter with a phase that is conjugate to $\mathbf{T}_{\tilde{\omega}_1}$ ($\mathbf{T}_{\tilde{\omega}_2}$) for $\omega<\Omega_L$ ($\omega>\Omega_L$). Although this obvious choice of $H(\omega)$ is not necessarily the true optimum, it does a good job in enhancing the polarization when the overlap of the $\mathbf{T}_{\tilde{\omega}_1}$ and the $\mathbf{T}_{\tilde{\omega}_2}$ functions is small, as in Fig. 5.

Computed results for the coherent polarization are shown in Fig. 6. To prevent aliasing effects, the 256-point $H(\omega)$ and $E_{\mathrm{in}}(\omega)$ vectors are first stretched by a factor of 8, with each point in the original vectors becoming 8 identical points in the stretched functions. The coherent polarization is then calculated from Eq. (9) by numerical integration. Figures 6(a) and 6(c) show the input (unshaped) laser pulse and the resultant induced polarization, respectively. As expected, the polarization turns on at $t=0$ and then oscillates with a constant amplitude at frequency ω_{21}. Figures 6(b) and 6(d) show the intensity profile of our derived waveform based on Eq. (18) and the corresponding coherent polarization, respectively. The computed polarization does indeed build up to a strong peak at 2.5 ps, as designed; the amplitude of the peak is enhanced by a factor of 3.03 compared with the no-pulse-shaping case. For $t>2.5$ ps the polarization decreases again to approach the same terminal level as in the no-pulse-shaping case. Similar enhancements are observed for other values of the delay τ in the

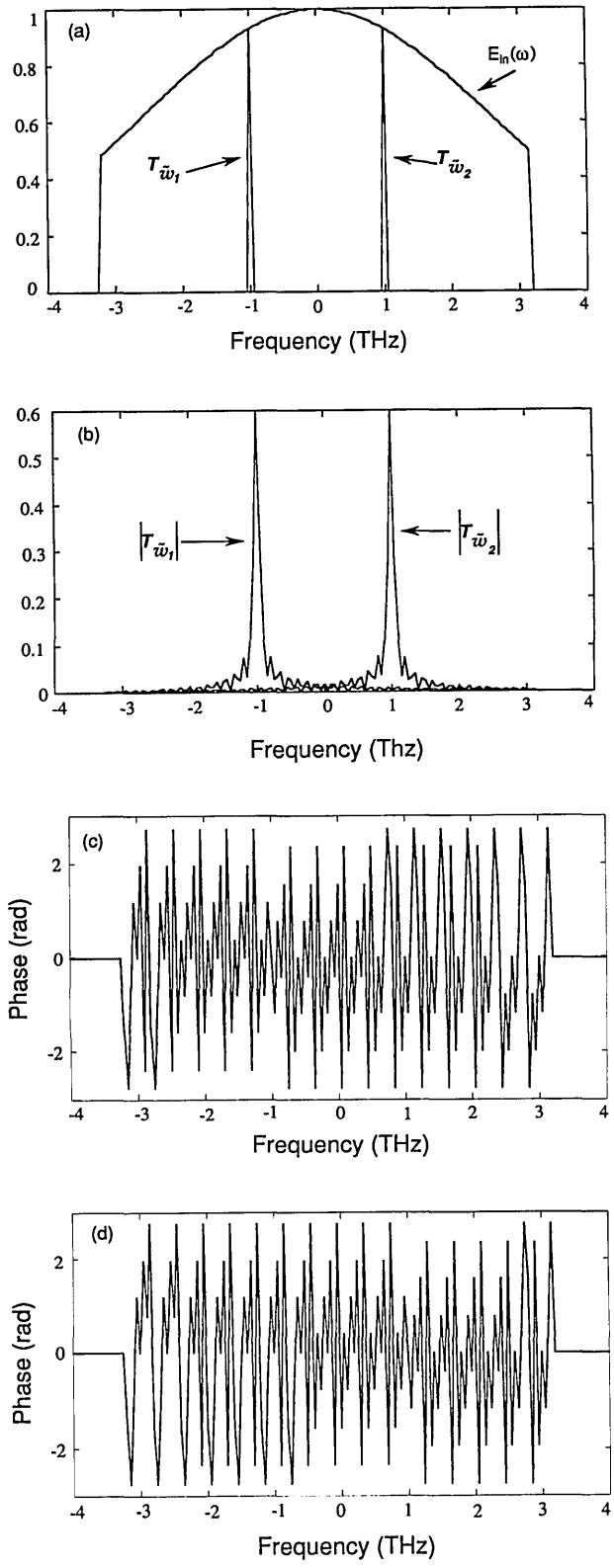

Fig. 5. Computed values of the $\mathbf{T}_\omega(\tau)$ operator. (a) For $\tau \to \infty$ the individual rows of $\mathbf{T}_\omega$ become delta functions, with amplitudes being determined by the input laser spectrum $E_{\text{in}}(\omega)$. The delta functions pictured ($\mathbf{T}_{\tilde{\omega}_1}$ and $\mathbf{T}_{\tilde{\omega}_2}$) are the rows of $\mathbf{T}_\omega$ evaluated at the conduction-subband energies $\tilde{\omega}_1$ and $\tilde{\omega}_2$. The input laser spectrum, which is clipped by a spectral window within the pulse shaper, is also shown. (b) For finite τ (2.5 ps in this case), $\mathbf{T}_{\tilde{\omega}_1}$ and $\mathbf{T}_{\tilde{\omega}_2}$ broaden; this effect permits enhancement of the peak polarization through pulse shaping. (c) Phase of $\mathbf{T}_{\tilde{\omega}_1}$. (d) Phase of $\mathbf{T}_{\tilde{\omega}_2}$.

range of several picoseconds. As an additional example, Figures 7(a) and 7(b) show the optimum pulse shape designed for a delay $\tau = -2.5$ ps and the corresponding in-

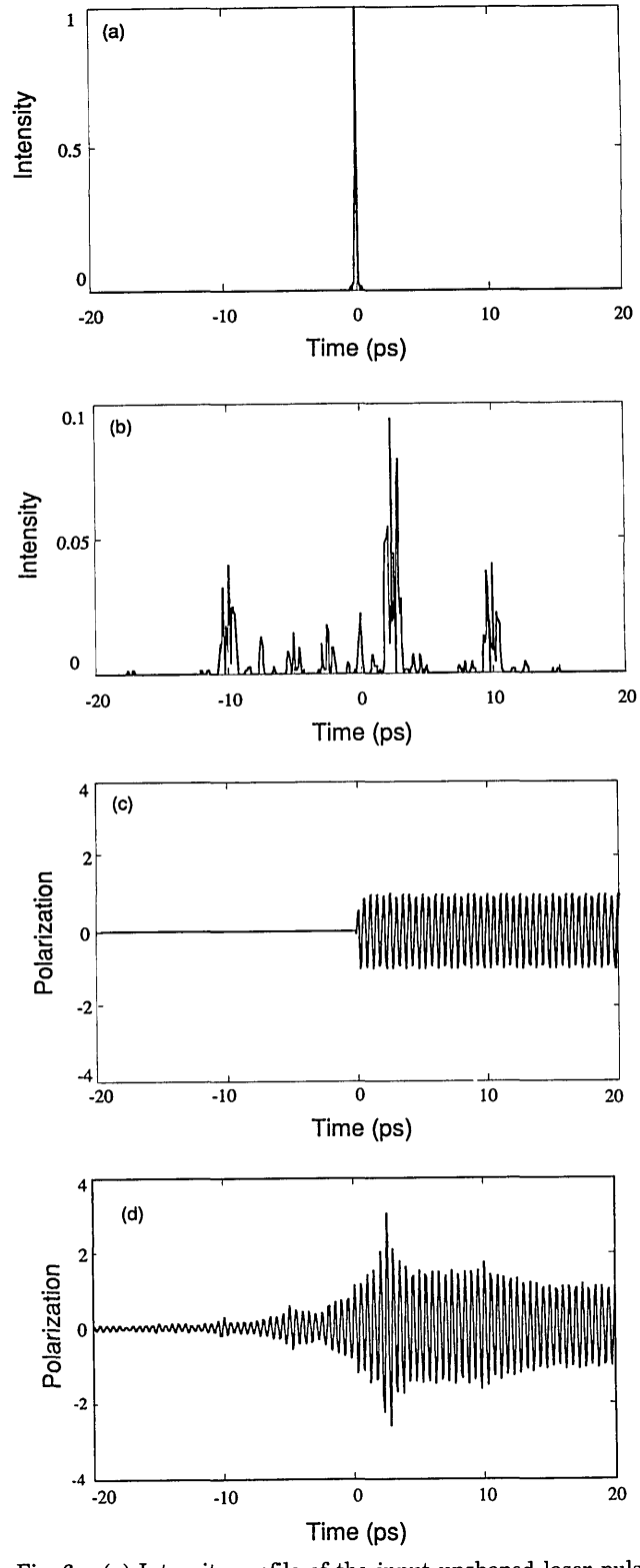

Fig. 6. (a) Intensity profile of the input unshaped laser pulse (normalized to unity). (b) Intensity profile of the shaped laser pulse (design 1). (c) Coherent polarization resulting from the unshaped laser pulse. The terminal polarization is normalized to unity. (d) Coherent polarization resulting from the shaped laser pulse. The amplitude peaks at $t = 2.5$ ps and is enhanced by a factor of 3.0 compared with (b).

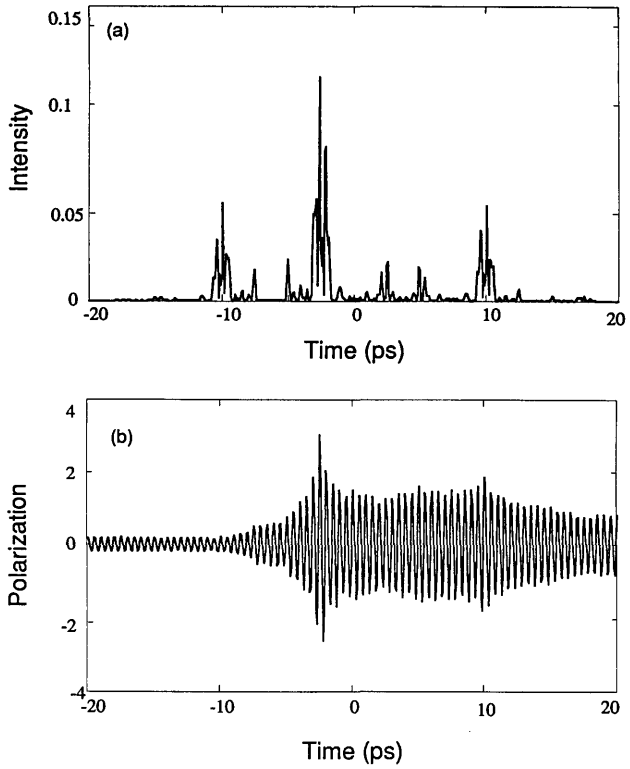

Fig. 7. Intensity profile of the shaped laser pulse (design 2). This is similar to the case shown in Fig. 6, but now the waveform is designed to give a peak polarization at $t = -2.5$ ps. (b) Resulting coherent polarization, again showing a threefold enhancement.

duced polarization, respectively. Except for the fact that the field and the polarization peaks are now moved to -2.5 ps, the resemblance to Fig. 6 is striking.

These theoretical results already indicate that it may be possible to apply pulse shaping and ultrafast coherent control to enhance charge motions in DCQW's. The prescribed laser pulses, although complicated, should be attainable by use of existing pulse-shaping technology. One difficulty, however, is that the waveforms shown in Figs. 6 and 7 extend over ~20 ps, a time that is long compared with the characteristic dephasing time. To realize real enhancements through pulse shaping, the resulting laser waveforms should be as short as the dephasing time. Next we discuss several modifications to the present calculation procedure that will enable us to obtain shorter optimum pulse shapes.

One strategy involves using a modified truncation (TR) operator in calculating $\mathbf{T}_\omega$. The modified truncation operator, which we denote $\mathbf{TR}'$, includes a Gaussian time window function and is written as

$$\mathbf{TR}'_{jk}(\tau) = \begin{cases} \exp(-t^2/\tau_w{}^2\delta_{jk}) & \text{for } t_j \le \tau \\ 0 & \text{for } t_j > \tau \end{cases}. \qquad (19)$$

Here τ_w, which we are free to choose, is a measure of the width of the Gaussian time window. The motivation is that, by including the Gaussian window, our calculations may provide waveforms that are better localized near $t = 0$. A similar time window arises physically in Fourier-transform pulse shaping because of the finite Gaussian spot sizes of the frequency components focused at the mask.[25,29] This effect sets the spectral resolution of the pulse shaper and leads to a time window roughly equal to the inverse spectral resolution. Typically the time window is of the order of tens of picoseconds, although windows of a few hundred picoseconds should be possible.

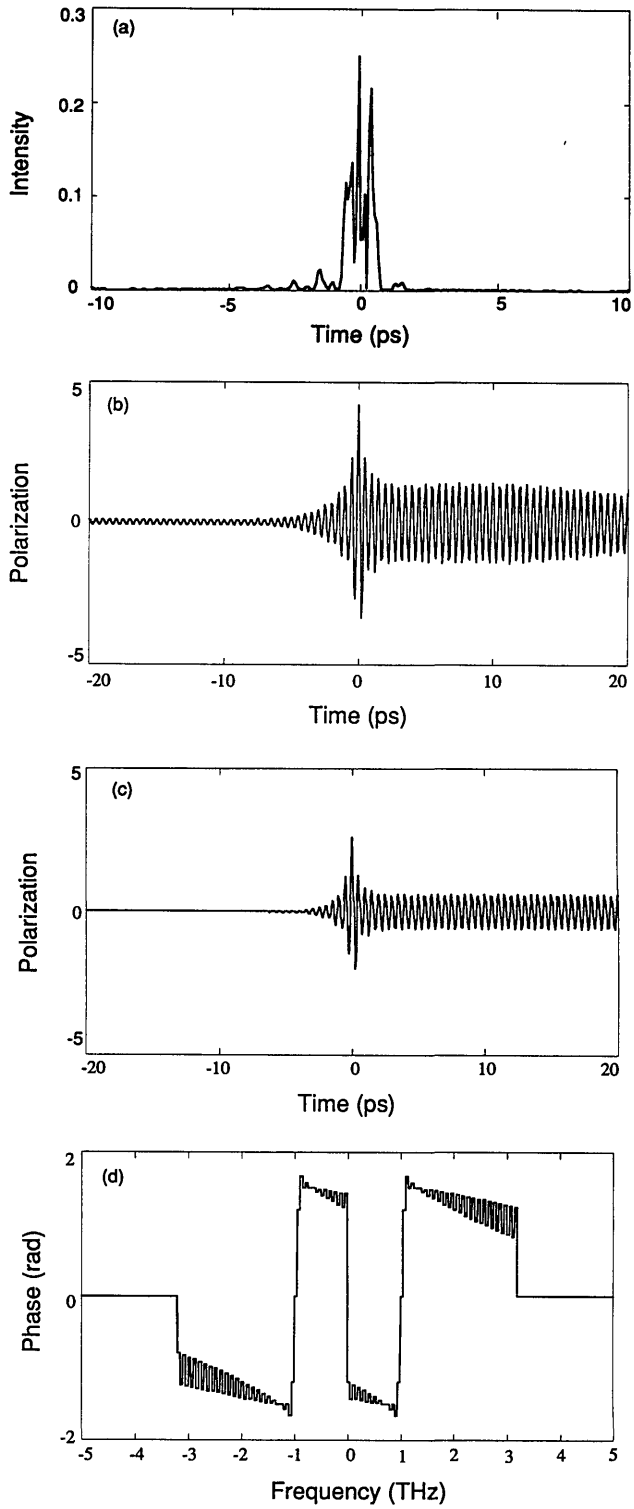

Fig. 8. (a) Intensity profile of the shaped laser pulse (design 3). (b) Resulting coherent polarization, showing a 4.2-fold enhancement at $t = 0$. (c) Coherent polarization resulting when the shaped laser pulse is multiplied by a 10-ps Gaussian to account for the finite spot sizes within the pulse-shaping setup. (d) Phase of the pulse-shaping filter.

The calculated results are shown in Fig. 8. The window parameter in **TR**′ corresponds to a Gaussian with a FWHM intensity duration of 10 ps, and the optimization occurs at $\tau = 0$. Otherwise the parameters used were the same as for Fig. 6. The intensity profile of the shaped pulse, Fig. 8(a), is still complicated but is now contained within a few picoseconds of $t = 0$. The shorter duration of the shaped pulse should make it much less sensitive to dephasing effects. The coherent polarization, Fig. 8(b), has a strong pulse at $t = 0$; the enhancement compared with the no-pulse-shaping case is now increased to 4.17. Note that, although a Gaussian window is assumed for calculating $H(\omega)$, no window is used in computing $P(t)$ in Fig. 8(b). If the shaped laser pulse is indeed multiplied by a 10-ps Gaussian before calculation of $P(t)$, Fig. 8(c) results. The polarization is still strongly peaked; however, both the peak and the level at large time values are reduced because multiplying by the time window does cut out some laser energy. Nevertheless, the peak is still 2.61 times larger than the steady-state polarization without pulse shaping. Finally, note that in this example the phase of the optimum filter, plotted in Fig. 8(d), is much smoother than in the previous case.

Another strategy for designing temporally localized pulse shapes is to increase the frequency spread δf per modulator pixel in the pulse-shaping setup. This decreases the maximum pulse duration attainable through spectral filtering. Figure 9 shows results for a calculation involving a 128-element phase modulator with $\delta f = 0.2$ THz. In this example the original truncation operator **TR** [Eq. (17c)] was used, with the target time set at $\tau = 0$. We actually model $H(\omega)$ as a 512-element vector, with each element corresponding to a frequency increment of 0.05 THz. The $\mathbf{T}_\omega$ matrix therefore has dimensions 512×512. After computing $\mathbf{T}_\omega$ we obtain a first cut at $H(\omega)$ by applying Eq. (18). We then group the $H(\omega)$ vector into 128 groups made up of 4 contiguous vector elements each, and within each group we reset $H(\omega)$ to the average of the 4 elements in the group. As a consequence our results apply to a 128-pixel modulator, and the need to pad each pixel to prevent time aliasing is built into the filter design calculations.

The intensity profile of the resulting shaped pulse is plotted in Fig. 9(a); most of the energy falls within ± 1 ps of $t = 0$. As a result polarization enhancements achieved with this waveform should be quite robust against dephasing. The peak in the coherent polarization at $\tau = 0$ is increased by a factor of 2.94 compared with the no-pulse-shaping case. Also, note that the averaging involved in setting the final filter results in an $H(\omega)$ value whose phase variation is quite smooth [Fig. 9(c)].

We can gain some insight by comparing the timing of the coherent polarization with that of the shaped electric field. The shaped field in this example is dominated by its real part, so in Fig. 10 the real part of the electric field and the polarization are plotted together. The field envelope is seen to oscillate at 1 THz, half the 2-THz charge oscillation frequency, as expected for a second-order process. Importantly, the field undergoes a dramatic π phase shift at $t = 0$. Thus the field initially oscillates nicely in phase, thereby causing $P(t)$ to grow to a strong peak at the target time. Directly after the peak the field changes sign, so that it immediately begins to de-

excite the polarization to reach the terminal polarization required by Eq. (10) and the initial power spectrum. It is remarkable that this purely mathematical filter design procedure results in shaped electric fields so amenable to simple physical interpretation.

5. DISCUSSION

A. Theoretical Issues

The present treatment so far indicates that it may be possible to use specially designed laser pulses to enhance the peak coherent polarization in DCQW's. However, two main theoretical issues remain for future research as follows:

First, the suggested laser waveforms, although good, are not necessarily globally optimum. It would be useful to establish limits that define how large an enhancement of the peak THz emission is possible in principle for a given set of laser, modulator, and sample parameters.

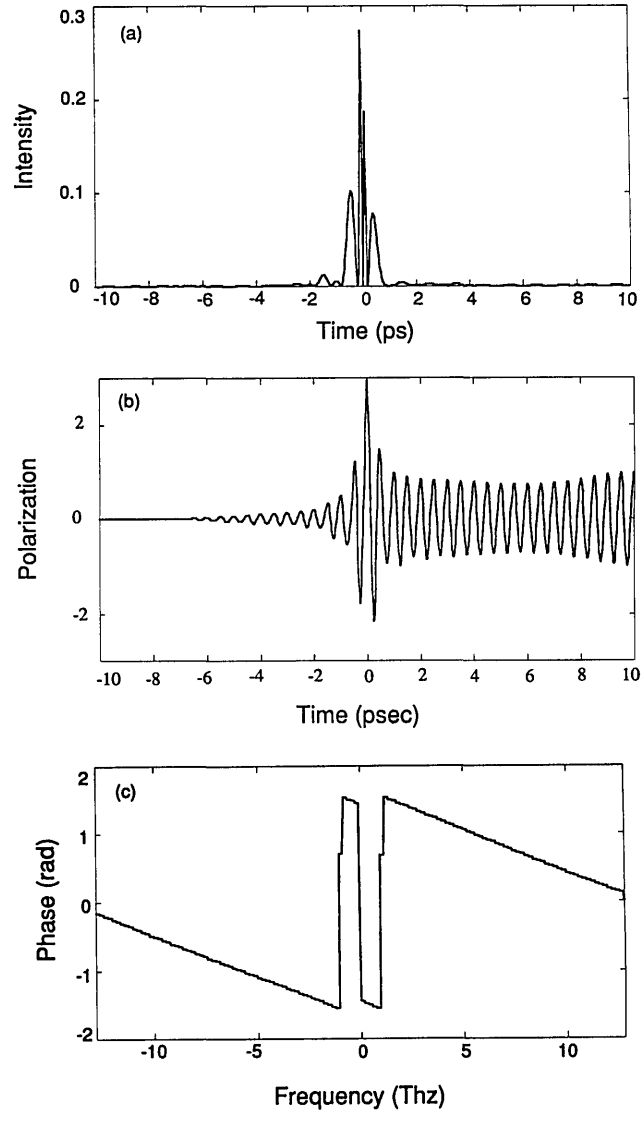

Fig. 9. (a) Intensity profile of the shaped laser pulse (design 4). Because most of the energy falls within ± 1 ps of $t = 0$, the polarization enhancement should be rather robust against dephasing. (b) Resulting coherent polarization, showing an enhancement of 2.9. (c) Phase of the pulse-shaping filter.

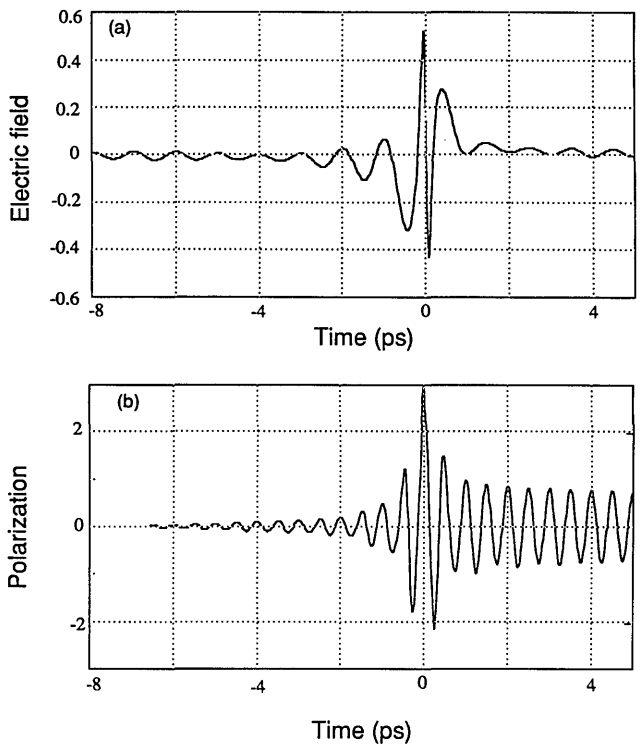

Fig. 10. (a) Real part of the electric field of the shaped laser pulse shown in Fig. 9. The imaginary part of the field is small in this example. Notice the π phase shift at $t = 0$: as soon as the polarization peak is achieved the laser field switches its phase and begins to drive the polarization back down. (b) Coherent polarization.

One might then use iterative optimization techniques, such as those reported in the coherent control literature,[9] to approach these limits. Additionally, one might seek to determine the laser and the modulator parameters (e.g., initial laser pulse width, number of modulator pixels, frequency span per pixel) for which the best optimization is possible.

Second, dephasing is ignored in the current study. This assumption is useful at present because it allows one to focus on the essential physics of shaped pulses and coherent charge oscillations. I have made some attempt to minimize the importance of dephasing by looking for suitable shaped pulses with durations less than or equal to the dephasing time. Nevertheless, in preparation for real experiments, one should calculate how dephasing affects the coherent polarization excited by the current shaped-electric-field designs and should calculate new laser waveforms that are optimum in the presence of dephasing.

Finally, in the current analysis only the coherent polarization $P(t)$ was calculated; the resulting THz radiation was not actually plotted. However, because the radiation is proportional to the second derivative of the oscillating dipole, by enhancing the coherent polarization one should also obtain an enhanced THz emission.

B. Additional Applications

Further prospects for coherent control in semiconductor heterostructures, with implications beyond those of the proposed DCQW studies, can also be envisaged. In particular, excitation with shaped ultrashort pulses may offer interesting possibilities for controlling the charge dynamics in multiple-well systems and superlattices.

In a two-well system an electron initially created in well 1 has no choices: it can tunnel only into well 2, and then it can return only to well 1, and so forth. Pulse shaping merely affects the amplitude of the induced charge oscillation. Multiple-well systems, consisting of three (or more) degenerate coupled quantum wells, offer new possibilities compared with two-well systems. In a three-well system an electron initially created in the leftmost well would initially tunnel into the adjacent central well, as before. At that point the electron now has several possibilities: it can return to the first well, it can tunnel to the rightmost well, or the wave function can split among the various wells. The probability that an electron will spend time in the rightmost well depends on the design of the three-well system and on the pulse shape. By exciting the sample with a properly chosen shaped laser waveform, one has the possibility of controlling the extent, if any, to which the electron becomes localized in the rightmost well. Thus, unlike for double-coupled-well systems, in a three-well system one has the truly exciting prospect of using coherent control to determine where the electron will go. Ultimately this could have novel device applications, e.g., for recognizing the presence of a particular ultrafast waveform.

Superlattices may also serve as an interesting coherent control laboratory. Recent experiments resulted in the observation of coherent charge oscillations (or Bloch oscillations[30,31]) after ultrashort pulse excitation of superlattices biased by applied electric fields.[6–8] These charge oscillations may be viewed as electron-wave-packet motion. By exploiting pulse shaping to optimize the phases and the amplitudes of the wave functions making up an electron wave packet, one has the possibility of manipulating the coherent charge oscillation, e.g., to optimize the induced dipole moment or radiation efficiency. Conversely, by studying the THz radiation for a series of different shaped laser waveforms one may perform spectroscopy to gain better understanding of the wave functions. This strategy would be similar to an approach proposed for teaching lasers to control molecules, in which experimental results are continuously fed into an iterative learning algorithm that then updates the laser waveform in an effort to meet some prespecified control objective.[12,32,33]

Finally, note that waveform design procedures similar to those outlined here could also prove useful for coherent control in simpler systems such as two-level atoms. For example, one could design pulse shapes that produce a transient peak in the upper-level population; this peak could significantly exceed the terminal population change permitted by the pulse area theorem. This temporary increase in the upper population might be exploited, e.g., to improve the yield in two-color, pulsed photoionization experiments.

6. SUMMARY

In this paper I have analyzed the charge oscillation amplitude achievable in degenerate coupled quantum wells excited by ultrashort light pulses. This analysis shows that, in the absence of dephasing, the terminal coher-

ent polarization obtained after the end of the pulse depends only on the optical power spectrum evaluated at the two conduction-subband energies. Therefore pulse shaping cannot enhance the terminal coherent polarization. In contrast, pulse shaping can lead to strong peaks in the oscillating dipole during the laser pulse. I have presented a methodology for designing ultrafast optical waveforms capable of producing strong peaks in the coherent polarization and have illustrated this approach by giving several examples. The computed results indicate the possibility of enhancing the peak oscillating dipole (and hence the resulting THz emission) by at least a factor of 4. Because our waveform designs can be generated by existing programmable pulse-shaping technology, experiments demonstrating the concepts described in this paper should be immediately feasible.

In a broader sense, these ideas point to the possibility of using specially designed multiple-quantum-well structures as a laboratory for testing coherent control concepts currently being explored in atomic and molecular systems. One advantage of a semiconductor coherent control laboratory would be the ability to tailor the Hamiltonian through the epitaxial growth process. In addition to two-coupled quantum-well systems, one can also seek to design special ultrafast laser waveforms to control the charge dynamics in systems with three or more wells or in superlattices. In multiple-well systems such investigations could lead to new possibilities for controlling the destination of photoexcited carriers and new concepts for using such semiconductor structures as recognition circuits for specific ultrafast waveforms. The use of shaped pulses to excite biased superlattices could lead to enhanced Bloch oscillations or improved knowledge of the superlattice wave functions.

ACKNOWLEDGMENT

The author is grateful to C. A. Bouman for suggesting the matrix approach central to Section 4.

REFERENCES

1. K. Leo, J. Shah, E. O. Gobel, T. Damen, S. Schmitt-Rink, W. Schafer, and K. Kohler, "Coherent oscillations of a wave packet in a semiconductor double-quantum-well structure," Phys. Rev. Lett. **66,** 201 (1991).
2. H. G. Roskos, M. C. Nuss, J. Shah, K. Leo, D. A. B. Miller, A. M. Fox, S. Schmitt-Rink, and K. Kohler, "Coherent submillimeter wave emission from charge oscillations in a double-well potential," Phys. Rev. Lett. **68,** 2216 (1992).
3. P. C. M. Planken, M. C. Nuss, I. Brener, K. W. Goossen, M. S. C. Luo, S. L. Chuang, and L. Pfeiffer, "Terahertz emission in single quantum wells after coherent optical excitation of light hole and heavy hole excitons," Phys. Rev. Lett. **69,** 3800 (1992).
4. P. C. M. Planken, I. Brener, M. C. Nuss, M. S. C. Luo, and S. L. Chuang, "Coherent control of terahertz quantum beats in a coupled quantum well using phase-locked optical pulses," Phys. Rev. B **48,** 4903 (1993).
5. I. Brener, P. C. M. Planken, M. C. Nuss, L. Pfeiffer, D. E. Leaird, and A. M. Weiner, "Repetitive excitation of charge oscillations in semiconductor heterostructures," Appl. Phys. Lett. **63,** 2213 (1993).
6. J. Feldmann, K. Leo, J. Shah, D. A. B. Miller, J. E. Cunningham, T. Meier, G. von Plessen, A. Schulze, P. Thomas, and S. Schmitt-Rink, "Optical investigation of Bloch oscillations in a semiconductor superlattice," Phys. Rev. B **46,** 7252 (1992).
7. K. Leo, P. H. Bolivar, F. Bruggemann, R. Schwedler, and K. Kohler, "Observation of Bloch oscillations in a semiconductor superlattice," Solid State Commun. **84,** 943 (1992).
8. C. Waschke, H. G. Roskos, R. Schwedler, K. Leo, H. Kurz, and K. Kohler, "Coherent submillimeter-wave emission from Bloch oscillations in a semiconductor superlattice," Phys. Rev. Lett. **70,** 3319 (1993).
9. H. Rabitz and S. Shi, "Optimal control of molecular motion: making molecules dance," Adv. Mol. Vib. Coll. Dyn. **1A,** 187 (1991).
10. S. Rice, "New ideas for guiding the evolution of a quantum system," Science **258,** 412 (1992).
11. W. S. Warren, R. Rabitz, and M. Dahleh, "Coherent control of quantum dynamics: the dream is alive," Science **259,** 1581 (1993).
12. Y. J. Yan, B. E. Kohler, R. E. Gillilan, R. M. Whitnell, K. R. Wilson, and S. Mukamel, "Molecular control spectrometer," in *Ultrafast Phenomena VIII*, J.-L. Martin, A. Migus, G. A. Mourou, and A. H. Zewail, eds. (Springer-Verlag, Berlin, 1992), pp. 8–12.
13. P. Brumer and M. Shapiro, "Laser control of molecular processes," Annu. Rev. Phys. Chem. **43,** 257 (1992).
14. A. M. Weiner, D. E. Leaird, G. P. Wiederrecht, and K. A. Nelson, "Femtosecond pulse sequences used for optical control of molecular motion," Science **247,** 1317 (1990).
15. A. M. Weiner, D. E. Leaird, G. P. Wiederrecht, and K. A. Nelson, "Femtosecond multiple-pulse impulsive stimulated Raman scattering spectroscopy," J. Opt. Soc. Am. B **8,** 1264 (1991).
16. N. F. Scherer, R. J. Carlson, A. Matro, M. Du, A. J. Ruggiero, V. Romero-Rochin, J. A. Cina, G. R. Fleming, and S. A. Rice, "Fluorescence-detected wave packet interferometry: time resolved molecular spectroscopy with sequences of femtosecond phase-locked pulses," J. Chem. Phys. **95,** 1487 (1991).
17. J. S. Melinger, A. Hariharan, S. R. Gandhi, and W. S. Warren, "Adiabatic population inversion in I_2 vapor with picosecond laser pulses," J. Chem. Phys. **95,** 2210 (1991).
18. C. Chen, Y.-Y. Yin, and D. S. Elliott, "Interference between optical transitions," Phys. Rev. Lett. **64,** 507 (1990).
19. S. M. Park, S.-P. Lu, and R. J. Gordon, "Coherent laser control of the resonant enhanced multiphoton ionization of HCl," J. Chem. Phys. **94,** 8622 (1991).
20. A. M. Weiner, "Efficiency of coherent charge oscillations in semiconductor heterostructures induced by femtosecond pulse sequences," in *Annual Meeting*, Vol. 16 of 1993 OSA Technical Digest Series (Optical Society of America, Washington, D.C., 1993), p. 253.
21. C. Lin, M. G. Littman, H. Rabitz, and S. A. Lyon, "Optimally designed laser pulse shape for use in inhomogeneously broadened quantum wells," in *Annual Meeting*, Vol. 16 of 1993 OSA Technical Digest Series (Optical Society of America, Washington, D.C., 1993), p. 15.
22. P. R. Smith, D. H. Auston, and M. C. Nuss, "Subpicosecond photoconducting dipole antennas," IEEE J. Quantum Electron. **24,** 255 (1988).
23. M. van Exter and D. R. Grischkowsky, "Characterization of an optoelectronic terahertz beam system," IEEE Trans. Microwave Theory Tech. **38,** 1684 (1990).
24. M. S. C. Luo, S. L. Chuang, P. C. M. Planken, I. Brener, and M. C. Nuss, "Coherent double-pulse control of quantum beats in a coupled quantum well," Phys. Rev. B **48,** 11,043 (1993).
25. A. M. Weiner, J. P. Heritage, and E. M. Kirschner, "High-resolution femtosecond pulse shaping," J. Opt. Soc. Am. B **5,** 1563 (1988).
26. A. M. Weiner, D. E. Leaird, J. S. Patel, and J. R. Wullert, "Programmable shaping of femtosecond pulses by use of a 128-element liquid-crystal phase modulator," IEEE J. Quantum Electron. **28,** 908 (1992).
27. A. M. Weiner and D. E. Leaird, "Generation of terahertz-rate trains of femtosecond pulses by phase-only filtering," Opt. Lett. **15,** 51 (1990).
28. M. C. Wefers and K. A. Nelson, "Programmable phase and amplitude femtosecond pulse shaping," Opt. Lett. **18,** 2032 (1993).
29. R. N. Thurston, J. P. Heritage, A. M. Weiner, and W. J.

Tomlinson, "Analysis of picosecond pulse shape synthesis by spectral masking in a grating pulse compressor," IEEE J. Quantum Electron. **22,** 682 (1986).
30. F. Bloch, "Uber die Quantenmechanik der Elektronen in Kristallgittern," Z. Phys. **52,** 555 (1928).
31. L. Esaki and R. Tsu, "Superlattice and negative differential conductivity in semiconductors," IBM J. Res. Dev. **14,** 61 (1970).
32. R. S. Judson and H. Rabitz, "Teaching lasers to control molecules," Phys. Rev. Lett. **68,** 1500 (1992).
33. P. Gross, D. Neuhauser, and H. Rabitz, "Teaching lasers to control molecules in the presence of laboratory field uncertainty and measurement imprecision," J. Chem. Phys. **98,** 4557 (1993).